

## Studying the Earth at Night from CubeSats

Dee W. Pack, Brian S. Hardy  
 The Aerospace Corporation  
 2310 E. El Segundo Blvd, El Segundo, CA 90245; 310-336-5645  
 dee.w.pack@aero.org

Travis Longcore  
 University of Southern California  
 Watt Hall Room 204  
 Los Angeles, CA 90089; 213-821-1310  
 longcore@usc.edu

### ABSTRACT

This paper presents examples of the latest imaging data of the Earth at night from multiple CubeSat platforms. Beginning in 2012, with AeroCube-4, The Aerospace Corporation has launched multiple CubeSat platforms in different orbits equipped with a common suite of CMOS sensors. Originally designed as utility cameras to assist with attitude control system studies and star sensor development, we have been using these simple camera sensors to image the Earth at night since 2014. Our initial work focused on observing nighttime urban lights and global gas flare signals at higher resolution than is possible with the VIIRS sensor. To achieve optimum sensitivity and resolution, orbital motion is compensated for via the use of on-board reaction wheels to perform point-and-stare experiments, often with multiple frame exposures as the sensor moves in orbit. Ground sample distances for these systems range from approximately 100 to 130 meters for the narrow-field-of-view cameras, to 500 meters for the medium-field-of-view cameras. In our initial work, we demonstrated that CMOS sensors flown on AeroCube satellites can achieve a nighttime light detection sensitivity on the order of  $20 \text{ nW}\cdot\text{cm}^{-2}\cdot\text{sr}^{-1}$ . This resolution and sensitivity allows for detection of urban lighting, road networks, major infrastructure illumination, natural gas flares, and other phenomena of interest. For wide-area surveys, we can also program our cameras to observe regions of interest and co-add pixels to reduce the data bandwidth. This allows for a greater number of frames to be collected and downloaded. These results may then be used to task later satellite passes. Here, we present new examples of our nighttime Earth observation studies using CubeSats. These include: 1) detecting urban growth and change via repeat imaging, 2) investigating the utility of color observations, 3) spotting major sources of light pollution, 4) studying urban-wildland interface regions where lighting may be important to understanding wildlife corridors, 5) imaging lightning and cloud cover at night using wide-area imaging, 6) observations of the very bright lights of fishing boats, and 7) observing other interesting natural phenomenon, including airglow emissions, and the streaking caused by proton strikes in the South Atlantic Anomaly. Our ongoing work includes utilizing a diversity in overpass times from multiple satellites to observe nighttime scenes, imaging high-latitude cities not optimally accessed by the international space station's cameras, and building a catalogue of observations of rapidly developing megacities and global infrastructure nodes. Data from CMOS sensors flown in common on 5 different AeroCubes in 4 different orbits have been collected. Our results show that enhanced CubeSat sensors can improve mapping of the human footprint in targeted regions via nighttime lights and contribute to better monitoring of: urban growth, light pollution, energy usage, the urban-wildland interface, the improvement of electrical power grids in developing countries, light-induced fisheries, and oil industry flare activity. Future CubeSat sensors should be able to contribute to nightlights monitoring efforts by organizations such as NOAA, NASA, ESA, the World Bank and others, and offer low-cost options for nighttime studies.

### 1.0 INTRODUCTION

Satellite monitoring of visible emissions at night has evolved into a useful capability for environmental monitoring and mapping the global human footprint. Pioneering work with Defense Meteorological Support Program (DMSP) sensors has been followed in recent years by studies using the Visible Infrared Imaging

Radiometer Suite (VIIRS) day-night band (DNB), and International Space Station (ISS) nighttime photography.<sup>1-9</sup> This is our second paper describing the use of simple CMOS cameras on small form CubeSats to image the Earth at night. In our prior work, we demonstrated point-and-stare experiments to achieve optimum sensitivity and resolution and showed our

ability to detect city lights and oil industry gas flares at ground sample distances varying from 100 to 500 m.<sup>10</sup> These data were compared to VIIRS data taken nearly simultaneously to show that the simple CMOS cameras achieved a nighttime detection sensitivity of approximately  $20 \text{ nW-cm}^{-2}\text{-sr}^{-1}$  with a SNR of approximately four.<sup>10</sup> This sensitivity approaches that specified by past work by Elvidge and co-workers proposing use of a Nightsat for studying global urban growth and related nighttime missions.<sup>11</sup> Guided by past research with both VIIRS and the ISS nightpod camera, we imaged bright, cloud-free cities in the Middle East, as well as New York-Philadelphia, Chicago, Osaka, and Beijing-Tianjin.

In this paper, we continue the use of identical cameras on related AeroCube spacecraft to further study the Earth at night. We present sample data on: changing light patterns over time due to urban growth, color changes in light due to LED introduction, light mapping at the urban-wildland interface in the Los Angeles region, and observations of major light pollution sources. We also demonstrate novel observations of severe weather at night from AeroCube platforms orbiting over Texas and Singapore, operations in the South Atlantic anomaly, and sample imagery of high-latitude cities.

We have at our disposal several different CubeSat platforms. The AeroCube-4 satellite, launched in 2012, is the oldest. Magnetometer issues and the lack of a rate gyro limit its utility for reliable nighttime imaging. We attempted some nighttime use of a follow-on satellite, AeroCube-4.5, but reduced storage capacity of its aging batteries limited our ability to use its rate gyro to maintain pointing into eclipse during nighttime collections. Used in our initial paper, AeroCube-5 has continued to perform well for nighttime imaging, but possesses only a NFOV camera. Two newer platforms, AeroCube-8C&D, have both MFOV and NFOV cameras, and have been used to demonstrate chasing transient weather phenomena, such as severe lighting, and to image selected nighttime scenes. All the work described in this paper used the AC-5 and AC-8 1.5U CubeSats equipped with GPS, Earth, Sun, and magnetic field sensors, and a rate gyro. When functioning properly, the ACS systems allows pointing with accuracy of approximately 1 degree, and allows for flexible pointing control of the onboard cameras. The AC-5 satellite flies in an orbit of: 450x900 km, 120° inclination. The AC-8C and D satellites fly in orbits of: 550x580 km, 98° inclination, with local time descending node of approximately 10:30 am. These orbital parameters allow us to access higher latitudes than the ISS (which is at 51.6° inclination) and overpass times that differ from the early morning

nighttime collections by the VIIRS DNB sensor onboard the Suomi spacecraft. These small spacecraft add to the assets available for nighttime study, offering flexibility for researching the Earth at night, but with the limitations imposed by the small optics and limited downlink in the current generation of AeroCubes. Table 1 reviews the performance parameters of the small cameras on-board our current CubeSats.

**Table 1. AeroCube Camera Suite Parameters**

Satellite (Camera)	Lens F#	Lens FL (mm)	Pixel Pitch (μm)	Nominal Altitude (km)	GSD (m)
AC-4, AC-8 (MFOV)	2	3.40	2.80	600	494
AC-5, AC-8 (NFOV)	2	15.8	2.80	600	106

The camera sensor chips in AC-4, AC-5, and AC-8 were ON Semiconductor MT9D131 1600x1200 pixel 10-bit color RGB Bayer pattern CMOS arrays. These chips are very compact, reasonably low-noise devices with decent low light sensitivity. Based on the manufacturer’s specifications, the quantum efficiencies for the RGB channels peak at 37%, and the full width at half maximum (FWHM) band pass for all three channels is approximately 400-850 nm. The individual channels are: R=560-850 nm, G=480-590 nm, B=400-512 nm FWHM. These cameras were included on the AC-4, AC-5, and AC-8 missions to provide daytime imagery of geographical features for calibration of the attitude-control system and were neither designed nor calibrated with a dedicated science mission in mind. Autoexposure was the only camera mode available in flight software for operations, and the images were downlinked after applying JPEG compression.<sup>10</sup> Additional information on these CubeSats has been summarized in several papers by Rowen, Gangestad and co-workers.<sup>12-15</sup> Despite their limitations, we have shown these tiny cameras can take nighttime images of city lights, oil industry gas flares, and other nighttime emission sources, particularly when tasked to point and stare at a target location, which improved the resolution and sensitivity.<sup>10</sup>

## 2.0 CUBESAT OBSERVATIONS AT NIGHT

We have investigated several ways of using the AeroCube CMOS cameras for nighttime imaging. As described above, all cameras share the same 1600x1200 pixel CMOS sensor, but have different focal length  $f/2$  lenses. The satellites flown to date have been in elliptical orbits. At nominal altitudes of 600km, the focal plane nadir footprints are approximately 790x590 km and 170x130 km for the MFOV and NFOV cameras, respectively. The NFOV cameras allow for

large urban regions to be viewed in one frame. The MFOV cameras are useful for surveys of larger regions, especially when used off-nadir. Initial work was performed using fly-and-shoot procedures, as in daytime imaging. We soon realized that the same pointing capability perfected during the development of the attitude control system of the AeroCube buses, originally for laser communication, could be applied to long-exposure remote sensing at night. We conducted a series of point-and-stare experiments in our prior paper<sup>10</sup> and some provide new nighttime examples of this technique in this work. Another capability that the CMOS chips possess is programmable, onboard pixel aggregation. By reprogramming our MFOV cameras to co-add 5x5 superpixels, we reduced the image sizes so that broad-area nighttime (and daytime) multi-frame videos of Earth scenes could be obtained and downlinked via the 200kbs RF communications link. Some single-frame examples of the use of this technique to capture lightning phenomenology, and to survey wide areas, are covered below and shown in video formats in the conference PowerPoint charts. JPEG compression is maximized for the survey videos and minimized for the higher quality full-resolution frames.

## 2.1 RUMAILA AND KUWAIT CITY

The Persian Gulf region has been a continued area of study for our nighttime AeroCube observations as it possesses many bright urban targets undergoing rapid development, a very large number of oil industry gas flare sites, and has generally favorable weather. Figure 1 shows two frames from a two-target, multi-frame, point-and-stare collection over the Northern Persian Gulf. The inset shows the map overlay of these frames. The AC-5 NFOV camera was commanded to take several frames of data while pointing at the Basra and Rumaila oil field region, and then shift to point at Kuwait City and take several additional frames of data. The two pictured adjacent frames from the two targeted regions are near nadir-pointed and stitch together well.

We first imaged this region with our AeroCube satellites in 2014 and have revisited the region to look for changes in the nighttime lights and oil industry activity. No major changes in gas flaring were observed in the Rumaila field or the nearby Kuwaiti areas. Kuwait City did show some subtle changes in the nighttime lights. Figure 2 shows the evolution of Kuwait City from 2013 to 2016 as observed by ISS photography<sup>16</sup> and our AeroCube satellite cameras. A coastal neighborhood expansion previously noted in prior imagery, now has lights filling out the entire area. Additionally, subtle lighting changes are noted in the Al Hishan region of Kuwait Bay. These are from construction of the 13-km Doha link bridge portion of

the ambitious Sheikh Jaber Al-Ahmad Al-Sabah Causeway project. The latter will span 36 km across Kuwait Bay and link Kuwait City to a massive planned development on Subiyah and Bubiyan Island on the country's Northern border. These are the type of urban infrastructure developments that are desirable to map with global nighttime lights monitoring in combination with daytime imaging. Our AeroCube sensors are approaching the sensitivities and resolutions appropriate for this kind of nighttime urban geographical study and mapping. Fast moving urban growth and infrastructure projects linking regions are increasing around the globe. These are important to monitor for economic and market research purposes. The increases in nighttime lights are also of interest for energy-use and light pollution research, including measuring the impact of waste light on ecosystems and human health.

## 2.2 MONITORING LOS ANGELES AT NIGHT WITH CUBESATS

We used the NFOV cameras on our AeroCube satellites to capture RGB color imagery of Los Angeles and surrounding areas. Two AC-5 camera images of the Los Angeles region (2015 and 2016) and one earlier ISS photography image (2010) illustrate the differences in field of view and resolution in Figure 3. The 2015 CubeSat image captured the Pacific Coast from Ventura County south to Los Angeles International Airport, including the brightest light source in the region, a massive greenhouse operation on the Oxnard Plain that operates during the winter months.<sup>17</sup> Nighttime-operating greenhouses are a growing source of light pollution around the globe.<sup>8</sup> The 2016 image shows full regional coverage of the Los Angeles metropolitan area, including much of the transportation network of freeways and well-lit major boulevards. Notable bright emissions are seen around the airport, harbor, downtown Los Angeles, the railyard to the southeast, and in commercial areas of Santa Monica, Hollywood, and Universal City. In comparison, the 2010 ISS photograph shows a smaller portion of the region at higher resolution. Comparison of the 2016 and 2010 imagery reveals evidence of conversion from yellow-orange high-pressure sodium lamps to much bluer full-spectrum LED lamps within the streetlight system of the City of Los Angeles, indicating the usefulness of these data in tracking global trends in street light conversion to full-spectrum LEDs.<sup>18,19</sup> The port and railyard areas continue to exhibit very bright yellow high-pressure sodium lighting. Another notable feature is the dark region of the Santa Monica Mountains, bisecting the City of Los Angeles. This range is home to an isolated population of mountain lions, including one individual in Griffith Park on the eastern end. We are using these data, in combination with VIIRS data, to

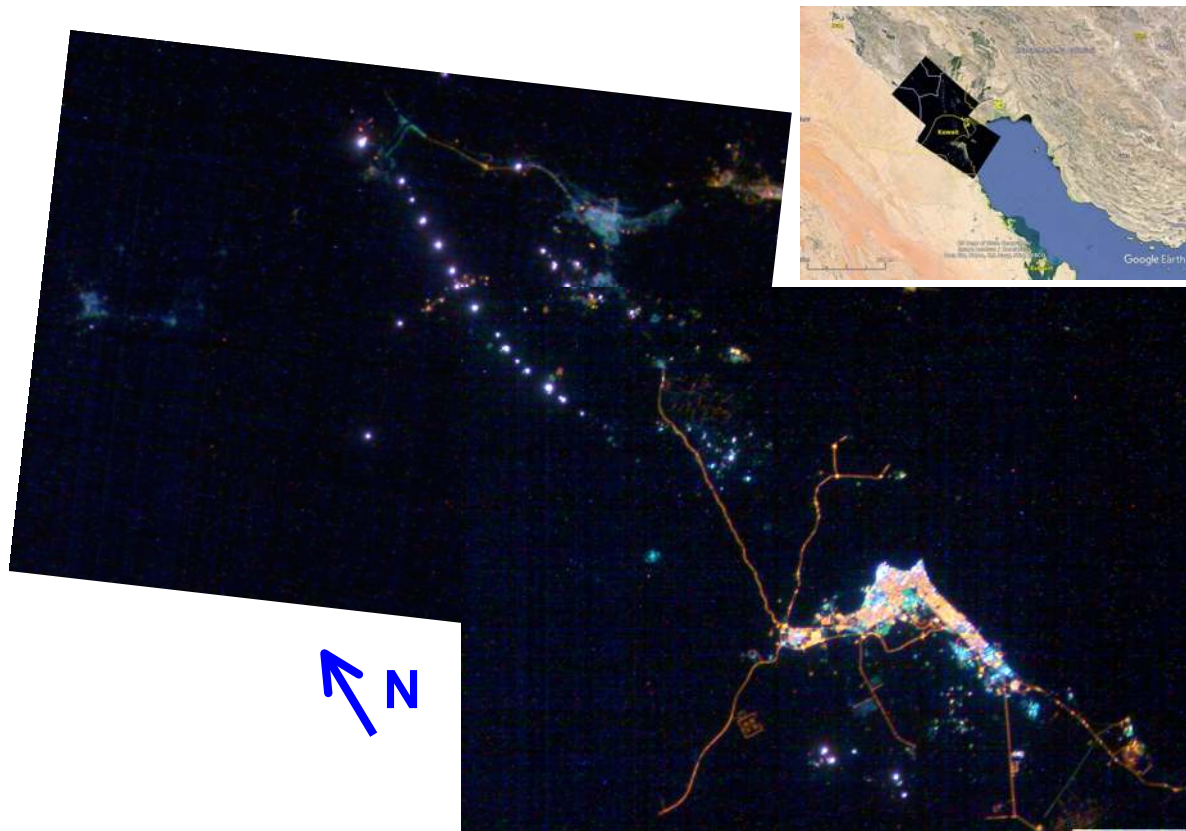


Figure 1. Two AC-5 images taken sequentially during a multi-frame collection over the Basra and Rumaila gas flare region and Kuwait City. 15 August 2016, 22:25:11 – 22:25:51 UT. The inset shows the regional overlay on Google Earth.

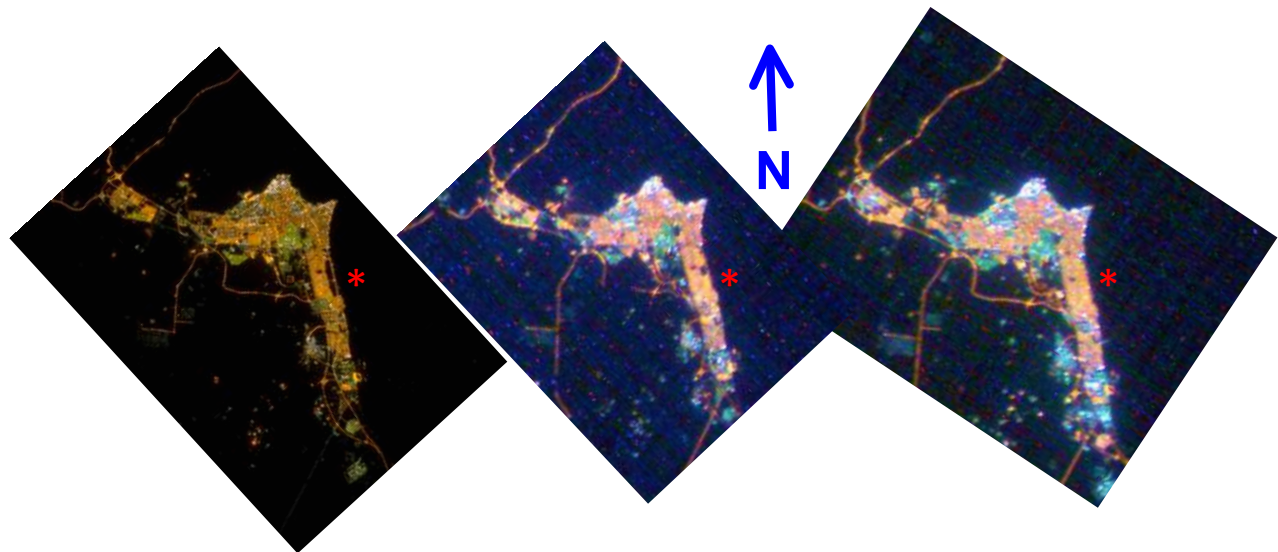


Figure 2. The development of a Kuwait coastal neighborhood (\*) is evident in this sequence of ISS and AC-5 data. Other subtle lighting changes also appear. From left to right: 12 Feb 2013 ISS Nikon 180 mm Lens ~ 20m GSD, 11 May 2015 AC-5 NFOV Camera ~ 130m GSD, 15 Aug 2016 AC-5 NFOV Camera ~ 130m GSD.



**Figure 3. Two AC-5 Images of the Los Angeles region and one ISS photo overlaid on Google Earth. From Left to right: 19 Sep 2015 AC-5 NFOV Camera ~ 130m resolution GSD, 22 Aug 2016 AC-5 NFOV Camera ~ 130m resolution, 30 Nov 2010 ISS Nikon with 180mm lens ~ 20 m GSD.**

describe a “darkest path” corridor through this urban-wildland interface that could help with species conservation and corridor planning in the Santa Monica Mountains ecosystem. Best-practice techniques of fusing color space camera data with the coarser VIIRS data are also being studied.

### 2.3 HOUSTON FLYBY: IMAGING LIGHTNING AND GULF COAST CITIES

Figure 4 shows selected AC-8 MFOV camera images from a 7-minute, 129-frame sequence as the satellite

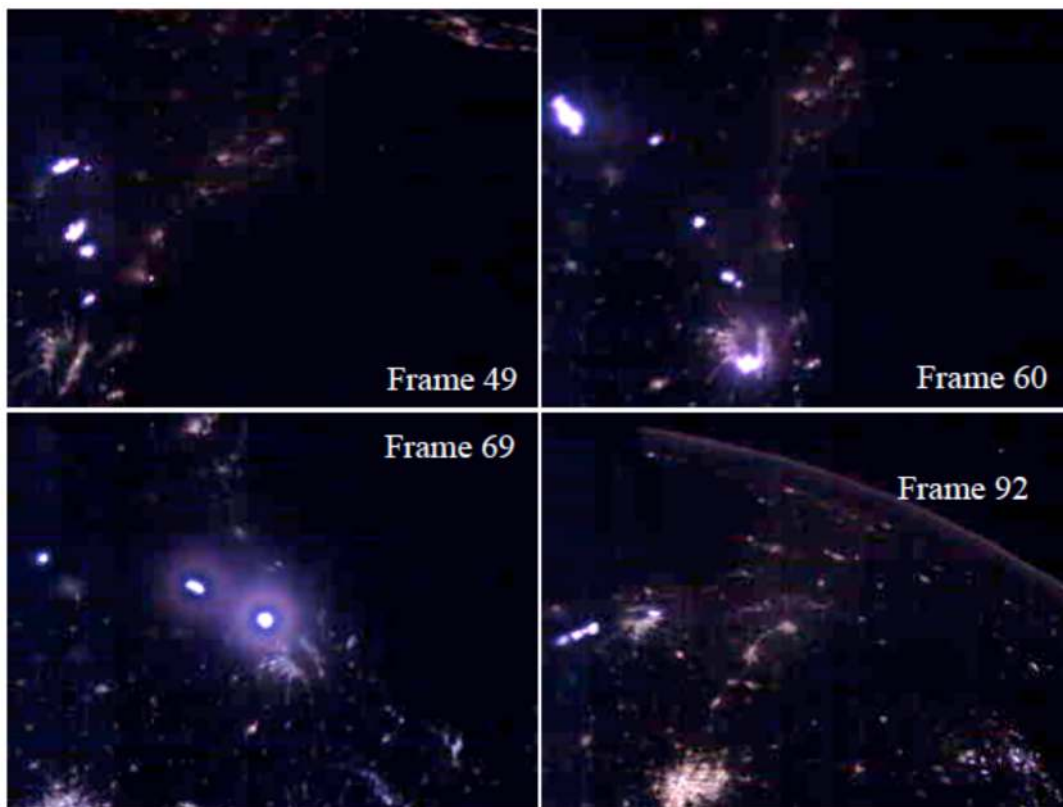


**Figure 4. Imaging Lightning with a CubeSat. AC8-C MFOV camera 5x5 aggregation mode 27 March 2017 16:29:41 UT. Four frames from a 129-frame sequence that images lightning activity from thunderstorms running northeast from Houston, TX which is partially obscured by unseen clouds. Frame 49 shows the Gulf Coast from Florida to Houston. Frame 60 shows Houston to New Orleans. Frame 69 is nadir-pointed at Houston, with Dallas coming into view. Frame 92 looks back towards Dallas, Houston, Austin and Fort Worth, with two prominent natural gas fields showing flare activity. The airglow layer is visible above the limb, as is a bright star. Bright lighting flashes are prominent in each image.**



orbited over the United States from the Gulf of Mexico on 27 March 2017 at 16:30UT. The Moon was at 50° elevation, 139° azimuth and 0% illuminated (new). The spacecraft was tasked to point at a front of developing severe thunderstorms along the Texas-Louisiana border. Four RF ground stations located in Florida, Texas, California and Hawaii are used to uplink commands and downlink telemetry and data from our CubeSat constellation. In this experiment, the pointing command sequence was uploaded from our Florida ground station 90 minutes prior to the data being collected over Texas. This is an example of our distributed ground station network allowing transient severe weather events to be targeted. The CMOS chip was programmed to reduce the 1600x1200 pixel frames via 5x5 aggregation to full-field-of-view 320x240 pixels, so more data could be collected, compressed onboard and downloaded via our 200 Mbps communications link. In the full-frame sequence, as the satellite orbits from the south, the Florida coast is readily visible, along with New Orleans and Baton Rouge, Louisiana, as well as Havana, Cuba, and Cancun and Merida, Mexico. As the satellite flies further north, Houston, Texas becomes visible, bisected by clouds (not visible) obscuring the city lights. A line of thunderstorms running to the Northeast are lit up by frequent very bright lighting bursts. Repeated localized bursts occur over Houston and Natchitoches. Dallas/Fort Worth comes into view and the cities of Austin and San Antonio as well as a band of gas flares to their south and a very large area of gas flaring in West Texas into New Mexico, as the satellite spins to look back from the north. This experiment confirmed our ability to target transient high-energy weather events, and that our techniques would be appropriate for other lightning remote sensing missions or future missions with additional sensors, such as gamma-ray detectors.

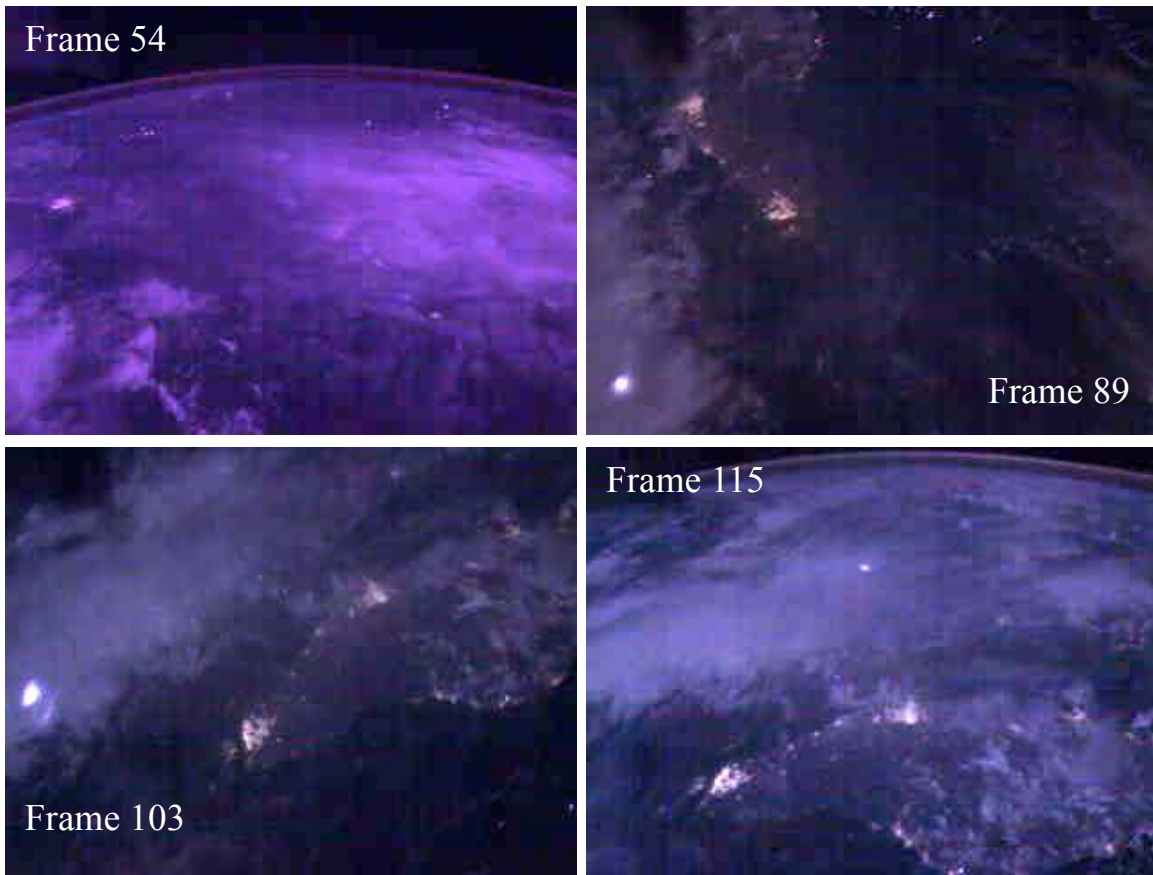
### **2.3 SINGAPORE FLYBY: IMAGING WEATHER AT NIGHT FROM A CUBESAT**

Figure 5 shows selected AC-8 MFOV camera images from an 8-minute, 160-frame sequence as the satellite orbits over Singapore, the Strait of Malacca and the Malay peninsula approaching from south of Java on 12 April 2017 at 16:06 UT. The spacecraft was tasked to point towards the lights of Singapore with the knowledge that thunderstorms were present in the area. By the time of the CubeSat overpass, Singapore was clear, but the region was quite cloudy with sporadic bright lightning events, including flashes that lit up significant portions of the observed scene at well above the already bright lunar illumination levels. The moon was at 57° elevation, 111° azimuth and 98% full. The camera images are again aggregated by 5x5 pixels. The sequence starts with

the satellite orbiting from the south with views of clouds over Java and Sumatra and cloud-covered Borneo in the distance. The lights of Singapore then come into view along with off-shore gas flares and Kuala Lumpur. The spacecraft then pivots to keep oriented towards Singapore and the Strait of Malacca. Georgetown comes into view as the fly-by sequence over the Malay peninsula moves towards completion. Lightning lights up entire cloud formations with sporadic high-altitude bursts being periodically visible. It is surprising how well such a small camera can see clouds at night in the visible band.

### **2.4 IMAGING FISHING VESSELS**

AC-8 MFOV cameras were used to take survey pictures around coastal zones in Asia, motivated by our interest in the growth of mega cities such as Shanghai, Seoul, and those in the Pearl River Delta region. We also wanted to study the ability of CubeSats to imaging fishing fleets. Figure 6 shows four images taken at the full 1600x1200 pixel resolution during a 4.5-minute, 27 frame collection sequence tasked over the East China Sea, the Sea of Japan, and Korea, which showed significant fishing boat activity. The data were taken on 29 April 2017 at 13:36 UT. The Moon was 14% illuminated but had set at the time of the observations (-8.2° elevation from Okinawa, -2.9° for Seoul). Frame 1 shows a line of boat lights running northeast across the East China Sea towards the Korean peninsula and Kyushu, with Okinawa visible to the south, and Shanghai to the east. Orbiting north, frame 11 brings a closer view of ships off Korea's Jeju island and in the Sea of Japan, some clustered so closely as to be unresolvable. Frame 19 continues north, and Seoul is prominently in view, as well as a band of darkness over North Korea. Subtle, dim clusters of lights appear northwest of Jeju Island and to the west of South Korea in the Yellow Sea. Frame 25 covers Seoul and North Korea, with views into China and the Bo Hai Gulf. Fishing lights have long been recognized in DMSP and VIIRS data. Recent global VIIRS data sets created by Baugh, Elvidge and co-workers have revealed the extent of industrial fishing practices in Asian waters, as well as other global zones.<sup>20</sup> Specialized algorithms have been designed for automated boat detection using VIIRS.<sup>21</sup> We were able to use our AeroCube sensors to detect these same signals readily in our first experiment of this type. VIIRS collected data over the same region during two passes at approximately 16:15 and 18:00 UT. A comparison between our data (from 13:36-13:40:30 UT) was made to the VIIRS boat detection data from the same night. This showed the AC-8 MFOV camera easily detected targets exhibiting VIIRS DNB levels above



**Figure 5. Imaging clouds and lightning over Singapore and the Strait of Malacca. AC8-C MFOV camera 5x5 aggregation mode 12 April 2017 16:06:44 UT. Four frames from a 160-frame sequence imaging weather over the Indonesian archipelago, Singapore, the Strait of Malacca and the Malay peninsula. Frame 54 shows lightning elevating the intensity of clouds over Borneo with the lights of Singapore and gas flares in the upper left of the image. The airglow layer is visible above the Earth limb. Frame 89 shows Singapore and Kuala Lumpur and lightning in clouds over Sumatra. Frames 103 and 115 show the view of the Malay Peninsula with more lighting as the satellite continues orbiting and points towards the Strait of Malacca.**

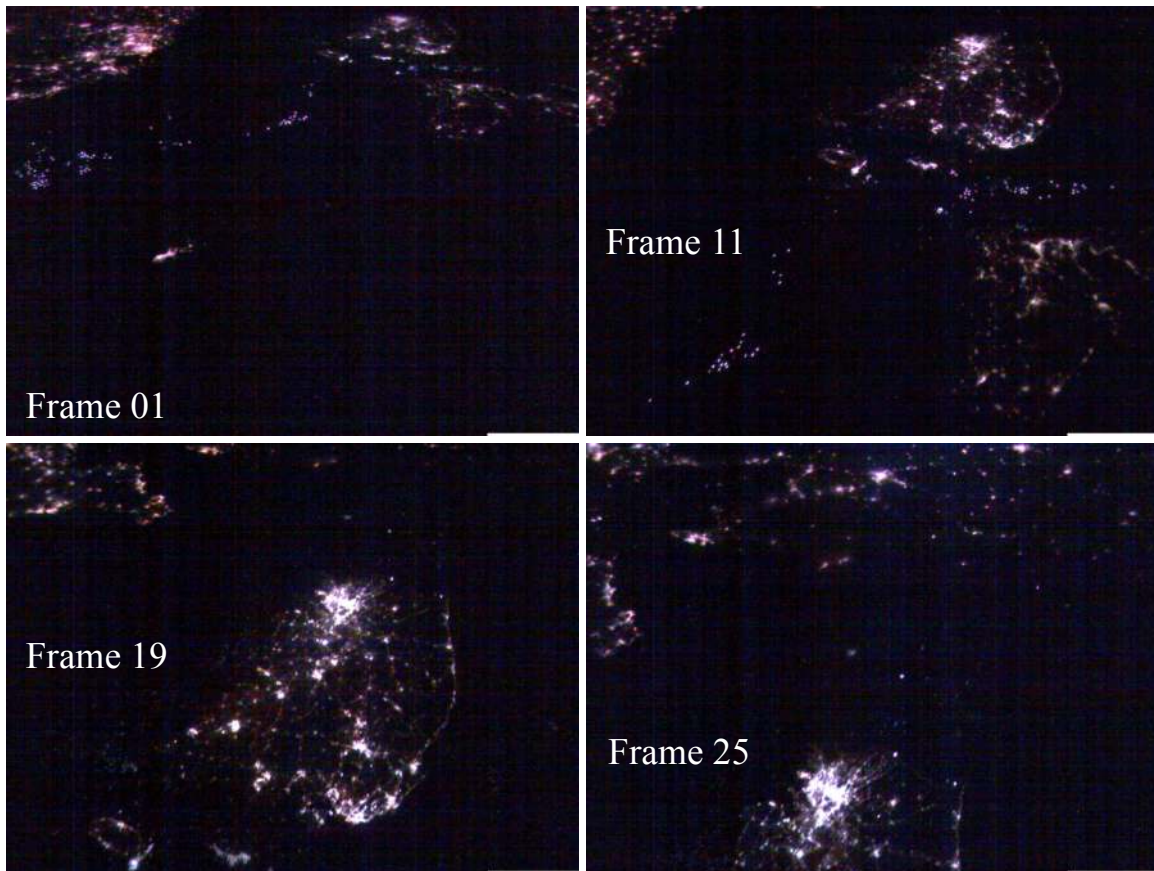


**Figure 6. Example use of a CubeSat for maritime domain awareness. AC-8D MFOV camera full resolution 29 April 2017 13:36:01 UT. Four frames from a 27-frame sequence covering the East China Sea traveling north over the Korean peninsula. Frame 1 shows ship lights north of Okinawa in the East China Sea running NE towards Korea and Kyushu. Frame 11 approaches South Korea and Jeju Island off its southern coast, with ships visible in the East China Sea and the Sea of Japan. Frames 19 and 25 continue the northward sequence as the lights of Seoul prominently appear.**

approximately  $80\text{-}100\text{ nW}\cdot\text{cm}^{-2}\cdot\text{sr}^{-1}$ , and just barely detected boat lights emitting at  $30\text{-}40\text{ nW}\cdot\text{cm}^{-2}\cdot\text{sr}^{-1}$  during this survey experiment. The subtle, dim clusters evident in frames 11 and 19 of Figure 6 corresponded to the dimmer illumination levels. This AC-8 collection did not maintain pointing quite as accurately as our AC-5 city lights experiments, as is evident from the minor streaking observed in the data, and the reduction in sensitivity. We have seen performance down to approximately  $10\text{ nW}\cdot\text{cm}^{-2}\cdot\text{sr}^{-1}$  for our AeroCube cameras under ideal conditions. VIIRS reports boat detections down to  $1\text{-}2\text{ nW}\cdot\text{cm}^{-2}\cdot\text{sr}^{-1}$ , well beyond the capabilities of our small sensors, and saw many more ships in the target region. Having extra measurements from CubeSats, even if not as sensitive, opens new possibilities including spotting activity at different times of night, detecting activity under different weather conditions, and potentially tracking target motion.

## **2.5 IMAGING RIO DE JANEIRO – DATA FROM INSIDE THE SOUTH ATLANTIC ANOMALY**

The high-energy particle flux within the South Atlantic Anomaly<sup>22</sup> is known to cause issues with remote sensing imaging. Operations in this region are avoided by some instruments, and special designs have been implemented for others, such as the VIIRS DNB.<sup>23</sup> We decided to acquire nighttime images of Rio De Janeiro during August 2016 and observed bright pixel responses and streaks from high-energy protons within this region. Figure 7 shows AC-5 nighttime imagery of Brazil, with adjacent frames from the same night and two different days depicted. Each image exhibits dozens of hot pixels from proton hits, with some appearing as obvious multi-pixel streaks. It is hard to distinguish all of the high-energy particle artifacts from bright nighttime light features in these compressed data without access to the original raw data frames. Comparing adjacent frames,



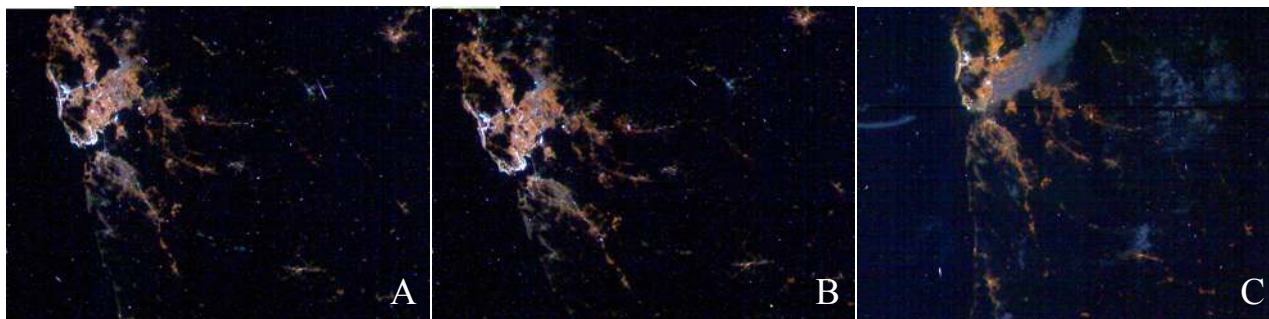


**Figure 7. AC-5 NFOV Camera. Three frames from two different days in the South Atlantic Anomaly imaging Rio de Janeiro. A) 08-29-16 04:31:33 UT Frame 1, B) 08-29-16 04:31:33 UT Frame 2, C) 08-18-16 02:51:23 UT Frame 4. Dozens of hot pixels due to proton strikes appear, including prominent streaks.**

or frames taken on different nights, helps sort out the artifacts. For the VIIRS DNB sensor, the challenge of operating within the SAA was largely overcome by the use of redundant focal planes.<sup>23</sup> Statistically-tested bright feature rejection algorithms are then used to clean up residual features.<sup>21</sup> For staring sensors, such as ours, similar bright feature, "spike" rejection algorithms could be used if carefully applied, but access to the raw frames would be a necessity.

### 3.0 CONCLUSIONS

The evolution of the AeroCube series of spacecraft has been focused on the perfection of the bus and attitude control system and on accommodating new technologies for rapid test and prototyping. The inclusion of a common suite of CMOS cameras has added greatly to the utility of AeroCube satellites. The same ability of these satellites to point and track, necessary for the focused goal of laser communication, was put to work imaging the Earth at night and studying the utility of small form spacecraft for nighttime missions. The flexibility of modern CMOS focal planes allows for automated modes of operation to be used with effect in both daytime and nighttime imaging of the Earth. The next generation of star-camera equipped AeroCube buses will have an even greater ability to point and perform useful remote sensing missions, including those identified in the NightSat Mission Concept<sup>11</sup> and other related work. In addition to the continuing evolution of small spacecraft and CMOS cameras, the solution of the communications downlink bottleneck by soon-to-be demonstrated laser communications systems, as well as by higher-bandwidth RF technologies, will also greatly contribute to the efficacy of these remote sensing missions. Higher-bandwidth communications will allow larger amounts of raw, uncompressed data to be downlinked, will increase the geographical coverage of nighttime studies, and will enable our small satellites to be "big data" contributors to Earth

science for more thorough scientific data exploitation.

### 4.0 FUTURE EFFORTS

CubeSats have been constructed and will soon be launched that will have more capable cameras on board. These include two OCS/AC-7 CubeSats and the ISARA CubeSat that hosts the CUMULOS payload. OCS is the NASA Optical Communications and Sensor Demonstration, also referred to as AeroCube-7.<sup>24</sup> ISARA is the JPL Integrated Solar Array and Reflectarray Antenna, a 3U CubeSat which hosts the CUBESAT MULTISpectral Observation System, an Aerospace Corporation sensor. All three of these CubeSats were scheduled to be launched last year but were delayed by launch issues. They are now scheduled to go into orbit no earlier than Fall, 2017. More details on these systems were tabulated in our prior paper.<sup>10</sup> CUMULOS was also discussed at the 2016 AIAA/USU Calibration Conference in August, and is also the subject of another paper in this conference along with the AeroCube-11 R3 sensor.<sup>25,26</sup> These new systems, as well as recently launched or proposed CubeSats designed by other researchers,<sup>27,28</sup> will bring additional space-based remote sensing resources to scientists exploring the nighttime Earth.

### Acknowledgments

This research was funded by The Aerospace Corporation's Independent Research and Development program. The authors also wish to acknowledge the U.S. Air Force Space and Missile Systems Center Advanced Development Directorate (SMC/AD) for their support of AeroCube payloads and the CUMULOS payload.

### References

1. Elvidge, C. D., Ziskin, D., Baugh, K. E., Tuttle, B. T., Ghosh, T., Pack, D. W., Erwin, E.

- H., Zhizhin, M., "A Fifteen Year Record of Global Natural Gas Flaring Derived from Satellite Data", *Energies*, vol. 2, no. 3, 2009.
2. Elvidge, C.D, Zhizhin, M., Baugh, K., Hsu, F.-C., Ghosh, T., "Methods for Global Survey of Natural Gas Flaring from Visible Infrared Imaging Radiometer Suite Data", *Energies*, vol. 9, January 2016.
  3. Miller, S.D, Mill, S.P., Elvidge, C.D., Lindsey, D. T., Lee, T.F., Hawkins, J.D., "Suomi Satellite Brings to Light a Unique Frontier of Nighttime Environmental Sensing Capabilities", *Proceedings of the National Academy of Sciences*, vol. 109, no. 39, September, 2012.
  4. Miller, S.D., Straka III, W., Mills, S., Elvidge, C., Lee, T., Solbrig, J., Walther, A., Heidinger, A., Weiss, S., "Illuminating the Capabilities of the Suomi National Polar-Orbiting Partnership (NPP) Visible Infrared Imaging Radiometer Suite (VIIRS) Day/Night Band", *Remote Sensing*, vol. 5, 2013.
  5. Elvidge, C.D.; Hsu, F.-C.; Baugh, K.; Ghosh, T., "Why VIIRS data are superior to DMSP for mapping nighttime lights", *Proceedings of the Asia-Pacific Advanced Network v. 35*, 2013.
  6. Elvidge, Christopher D., Mikhail Zhizhin, Feng-Chi Hsu, and Kimberly E. Baugh. "VIIRS nightfire: Satellite pyrometry at night." *Remote Sensing* 5, no. 9 (2013): 4423-4449.
  7. Elvidge, C.D.; Hsu, F.-C.; Baugh, K.; Ghosh, T., "National Trends in Satellite Observed Lighting: 1992–2012", In *Global Urban Monitoring and Assessment through Earth Observation*; Weng, Q., Ed.; CRC Press: Boca Raton, FL, USA, pp. 97–120, 2014.
  8. Kyba, C.C.M., Garz, S. Kuechly, H., De Miguel, S.A., Zamorano, J., Fischer, J., Hölker, F., "High-Resolution Imagery of Earth at Night: New Sources, Opportunities and Challenges", *Remote Sensing*, vol. 7, 1-23, January 2015.
  9. De Miguel, S.A.; Castaño, J.G.; Zamorano, J.; Kyba, C.C.M.; Pascual, S.; Ángeles, M.; Cayuela, L.; Martín Martínez, G.; Caltner, P., "Atlas of astronaut photos of Earth at night" *Astronomy and Geophysics*, vol. 55, no. 4 August 2014. This helpful Atlas to nighttime ISS photography is described by Kyba et. al. in reference 11 and online at: <http://www.citiesatnight.org>, and <http://www.nightcitiesiss.org/>
  10. Pack, D.W., Hardy, B.S. "CubeSat Nighttime Lights" *Proceedings of the AIAA/USU Conference on Small Satellites*, CubeSat Session IV: LEO Missions, SSC16-WK-44. 2016. <http://digitalcommons.usu.edu/smallsat/2016/S4LEOMis/1/>
  11. Elvidge, C.D, Cinzano, P., Pettit, D.R., Arvesen, J., Sutton, P., Small, C., Nemani, R., Longcore, T., Rich, C., Safran, J., Weeks, J, Ebener, S. "The Nightsat Mission Concept", *International Journal of Remote Sensing*, vol. 28, No. 12, May 2007.
  12. Rowen, D and Dolphus, R. 3-axis attitude determination and control of the AeroCube-4 cubesats. In *AIAA/USU Conference on Small Satellites, 10<sup>th</sup> Annual CubeSat Developers' Workshop*, 2013.
  13. Gangestad, J.W., Rowen, D.W. and Hardy, B.S., "Forest Fires, Sun glint, and a Solar Eclipse: Responsive Remote Sensing with AeroCube-4", *Geoscience and Remote Sensing Symposium (IGARSS)*, IEEE, Quebec City, Canada, July 2014.
  14. Gangestad, J.W., Rowen, D.W. and Hardy, B.S., "Along for the Ride: Experience with Flexible Mission Design for CubeSats", *Proceedings of the AIAA/AAS Astrodynamics Specialist Conference, SPACE Conferences and Exposition*, San Diego, CA, August, 2014.
  15. Gangestad, J.W., Rowen, D.W., Hardy, B.S. and Hinkley, D.A., "Flying in a Cloud of CubeSats: Lessons Learned from AeroCube-4, -5 and -6", *Proceedings of the 65 International Astronautical Congress*, Toronto, Canada, September, 2014.
  16. All photographs taken from the International Space Station and their meta data are available at "The Gateway to Astronaut Photography of Earth", which is run by NASA: <http://eol.jsc.nasa.gov>.
  17. (Longcore et al., unpublished analysis of VIIRS data).
  18. Aubé, M., J. Roby, and M. Kocifaj. 2013. Evaluating potential spectral impacts of various artificial lights on melatonin suppression, photosynthesis, and star visibility. *PLoS ONE* 8:e67798.
  19. Falchi, F., P. Cinzano, D. Duriscoe, C. C. Kyba, C. D. Elvidge, K. Baugh, B. A. Portnov, N. A. Rybnikova, and R. Furgoni. The new

- world atlas of artificial night sky brightness. *Science Advances* 2:e1600377. 2016.
20. Baugh, K.; Hsu, F.-C.; Elvidge, C.D.; Zhizhin, M. Nighttime lights compositing using the VIIRS day-night band: Preliminary results. *Proc. Asia Pac. Adv. Netw* **2013**, 35, 70–86.
  21. Elvidge, C.D.; Zhizhin, M.; Baugh, K.; Hsu, F.-C. Automatic Boat Identification System for VIIRS Low Light Imaging Data. *Remote Sens.* **2015**, 7, 3020-3036.
  22. Vernov, S.N.; Gorchakov, E.V.; Shavrin, P.I.; Sharvina, K.N. Radiation Belts in the Region of the South-Atlantic Magnetic Anomaly. *Space Sci. Rev.* 1967, 7, 490–533.
  23. Joint Polar Satellite System Visible Infrared Imaging Radiometer Suite Sensor Data Records Algorithm Theoretical Basis Document (ATBD) See: S-NPP/JPSS Science Documents. <http://www.star.nesdis.noaa.gov/jpss/Docs.php>, [https://ncc.nesdis.noaa.gov/documents/documentation/ATBD-VIIRS-RadiometricCal\\_20131212.pdf](https://ncc.nesdis.noaa.gov/documents/documentation/ATBD-VIIRS-RadiometricCal_20131212.pdf)
  24. Janson, S.W., Welle, R., Rose, T., Rowen, D., Hinkley, D., Hardy, B. La Lumondiere, S., Maul, G., Werner, N. “The NASA Optical Communication and Sensors Demonstration Program: Preflight Update”, Proceedings of the 29<sup>th</sup> Annual AIAA/USU Conference on Small Satellites, Logan, Utah, USA, August, 2015.
  25. Ardila, D., Pack, D.W., "The Cubesat Multispectral Observation System (CUMULOS)." *Conference on Characterization and Radiometric Calibration for Remote Sensing*, (2016). <http://digitalcommons.usu.edu/calcon/CALCON2016/all2016content/27/>
  26. Pack, D.W., et. al. “Two Aerospace Corporation CubeSat Remote Sensing Imagers: CUMULOS and R3” *Proceedings of the AIAA/USU Conference on Small Satellites*, 2017.
  27. Manzoni, G., Brama, Y.L., Zhang, M. 2016. “Athenoxat-1, Night Vision Experiments in LEO” *Proceedings of the AIAA/USU Conference on Small Satellites*, CubeSat Session IV: LEO Missions, SSC-16-WK-07. <http://digitalcommons.usu.edu/smallsat/2016/S4LEOMis/6/>.
  28. Walczak, K. 2016. “NITESat: A People-Powered Science Mission” *Proceedings of the AIAA/USU Conference on Small Satellites*, Poster Session III. <http://digitalcommons.usu.edu/smallsat/2016/Poster3/8/>.